

# Source Strengths of Ultrafine and Fine Particles Due to Cooking with a Gas Stove

LANCE A. WALLACE,\*†  
STEVEN J. EMMERICH,‡ AND  
CYNTHIA HOWARD-REED‡

U.S. Environmental Protection Agency,  
11568 Woodhollow Court, Reston, Virginia 20191, and  
National Institute of Standards and Technology,  
Gaithersburg, Maryland 20899

Cooking, particularly frying, is an important source of particles indoors. Few studies have measured a full range of particle sizes, including ultrafine particles, produced during cooking. In this study, semicontinuous instruments with fine size discriminating ability were used to calculate particle counts in 124 size bins from 0.01 to 2.5  $\mu\text{m}$ . Data were collected at 5 min intervals for 18 months in an occupied house. Tracer gas measurements were made every 10 min in each of 10 rooms of the house to establish air change rates. Cooking episodes ( $N = 44$ ) were selected meeting certain criteria (high concentrations, no concurrent indoor sources, long smooth decay curves), and the number and volume of particles produced were determined for each size category. For each episode, the particle decay rate was determined and used to determine the source strength for each size category. The selected cooking episodes (mostly frying) were capable of producing about  $10^{14}$  particles over the length of the cooking period (about 15 min), more than 90% of them in the ultrafine ( $<0.1 \mu\text{m}$ ) range, with an estimated whole-house volume concentration of  $50 (\mu\text{m}/\text{cm})^3$ . More than 60% of this volume occurred in the  $0.1\text{--}0.3 \mu\text{m}$  range. Frying produced peak numbers of particles at about  $0.06 \mu\text{m}$ , with a secondary peak at  $0.01 \mu\text{m}$ . The peak volume occurred at a diameter of about  $0.16 \mu\text{m}$ . Since the cooking episodes selected were biased toward higher concentrations, the particle concentrations measured during about 600 h of morning and evening cooking over a full year were compared to concentrations measured during noncooking periods at the same times. Cooking was capable of producing more than 10 times the ultrafine particle number observed during noncooking periods. Levels of  $\text{PM}_{2.5}$  were increased during cooking by a factor of 3. Breakfast cooking (mainly heating water for coffee and using an electric toaster) produced concentrations about half those produced from more complex dinnertime cooking. Although the number and volume concentrations observed depend on air change rates, house volume, and deposition rates due to fans and filters, the source strengths calculated here are independent of these variables and may be used to estimate number and volume concentrations in other types of homes with

widely varying volumes, ventilation rates, and heating and air-conditioning practices.

## Introduction

Fine particles have been linked to mortality and morbidity in scores of studies, but the exact causal agent is still unknown (1). One possibility is ultrafine particles (diameter  $<0.1 \mu\text{m}$ ), which usually form the bulk of particle number but contribute only negligibly to particle mass. They have been found in several animal studies to be more toxic than larger particles of the same composition (2).

Cooking with gas stoves has also been found in some studies to be associated with respiratory illness (3), although others have not found a relation. Although these studies linked the observed illnesses with the higher  $\text{NO}_2$  created by gas stoves, it may also be possible that ultrafine particles were partially or wholly responsible for the illnesses (4).

Studies of exposure to particles have shown that the major indoor source other than smoking is cooking, particularly frying or sautéing (5–8). To estimate the impact of this source, it would be desirable to understand the mean and range of cooking source strengths. Measured real-time particle concentrations due to cooking have been obtained in previous exposure studies (9–11), but source strengths could not be calculated because concurrent particle decay rates could not be determined for individual homes. These decay rates must be measured in conjunction with concentration measurements to determine source strengths. The estimated range and distribution of source strengths can then be used in modeling studies of indoor air quality.

A two-year study in an occupied town house has provided a large database on air change rates (12–13), particle decay rates (14–15), and concurrent particle concentrations (16). These measurements make it possible to determine the source strengths of cooking activities for a spectrum of particle sizes from ultrafine ( $0.01\text{--}0.1 \mu\text{m}$ ) to fine ( $2.5 \mu\text{m}$ ) particles.

Since the decay rates can only be determined for cases when particle number concentrations are quite high, our selected cooking episodes will be at the high end of the source strength distribution. To estimate the magnitude of the bias, we also investigate the number and volume concentrations associated with all types of cooking over an entire year (more than 500 h of cooking) and compare these values with the concentrations observed for our selected episodes.

## Experimental Section

The townhouse and instrumentation have been described fully in previous papers (12–16). Briefly, the townhouse is a four-bedroom house of three stories (basement, first floor, second floor) with a volume of about  $400 \text{ m}^3$ . A central fan circulates heated, air-conditioned, or untreated air through ductwork entirely contained in the conditioned area. The forced-air system uses 100% recirculated air. The kitchen has a laminated imitation wood surface. The living room, stairs, and bedrooms have hardwood floors with some area rugs. The basement and stairs leading to the basement are carpeted. During the experimental period, the house was occupied by two nonsmoking adults.

The stove is a gas stove with four top burners rated at 2600 W (9000 BTU/h) each and an oven with an upper gas burner (2900 W, 10 000 Btu/h) and a lower gas burner (5200 W, 18 000 Btu/h). An electric toaster was used for making toast in the mornings. The frying pan used for frying tortillas and eggs was well used (more than 30 years old) with a blackened copper bottom but a clean unmarked metallic

\* Corresponding author phone: (703) 620-4543; fax: (703) 860-0678; e-mail: wallace.lance@epa.gov.

† U.S. Environmental Protection Agency.

‡ National Institute of Standards and Technology.

frying surface. A range hood vented to the outdoors was present but not used during any of the cooking episodes reported here.

Particle monitoring instruments included a differential mobility analyzer (DMA) (model 3071, TSI, Inc., St. Paul, MN) linked to a condensation particle counter (CPC) (model 3010, TSI). Two nozzles were used alternately for about a month at a time. The smaller nozzle (0.471 mm) allowed a range of particle sizes to be studied between 10 and 450 nm in diameter. The larger nozzle (0.508 mm) covered a range of 18–1000 nm. Both nozzles were used throughout the year to provide information on the widest possible range of particle sizes. Each system included approximately 107 distinct particle sizes at equal intervals on a log scale. A 5 min cycle was chosen. The DMA–CPC is considered a reference instrument for determining sizes of particles but not necessarily the concentrations. Although the concentrations measured for ultrafine particles (<100 nm) agreed very well for the two nozzles, the large nozzle returned higher concentrations than the small nozzle for the overlap region between 100 and 445 nm (16). For the sake of consistency, in this study we included those measurements made using the small nozzle only.

The second instrument was an aerodynamic particle counter (APC) (aerodynamic particle sizer, model 3320, TSI). This instrument accelerates particles between two lasers, thus determining the aerodynamic diameter directly for particles in 50 size categories between 0.54 and 20  $\mu\text{m}$ . The APC was operated on a 1 min averaging time. Like the DMA–CPC, the APC returns a particle number concentration as the primary unit. It should be noted that the manufacturers have since discontinued the model used, because it was found to be undependable for particles larger than about 5  $\mu\text{m}$  (17). For that reason, no results are reported here for particles >2.5  $\mu\text{m}$ . Both particle instruments were located in the basement.

A third instrument was an optical particle counter (OPC) (model 500-I, Clime Instruments, Inc., Redlands, CA). The OPC is an optical scattering instrument with six custom size categories: 0.3–0.5, 0.5–1, 1–2.5, 2.5–5, 5–10, and >10  $\mu\text{m}$ . A pump with an airflow of 0.17  $\text{m}^3/\text{h}$  (0.1 cfm) was employed. This low-flow pump allowed an upper boundary of about  $2.8 \times 10^5$  particles/ $\text{m}^3$  to be measurable, compared to only  $2.8 \times 10^4$  particles/ $\text{m}^3$  for the standard 1.7  $\text{m}^3/\text{h}$  (1 cfm) pump. Concentrations often exceeded  $2.8 \times 10^4$  particles/ $\text{m}^3$ , but seldom reached  $2.8 \times 10^5$  particles/ $\text{m}^3$ . To avoid overloading the system optics and to extend the life of the instruments, the pump was operated for only 1 min of each 5 min period. This resulted in good number statistics for the three lowest size bins (<2.5  $\mu\text{m}$ ). Four such instruments were available, and were usually located outdoors and on each of the three floors of the townhouse. This instrument provided the only means of determining room-to-room differences, particularly between the source room and the other rooms.

The house's ventilation rate was measured continuously using the tracer decay method as described in ASTM Standard E741 (18) with sulfur hexafluoride ( $\text{SF}_6$ ) as the tracer gas and a gas chromatograph with electron capture detector (GC–ECD) detection system. Every 2–4 h a tracer gas ( $\text{SF}_6$ ) was injected into the return duct. The gas was sampled through polyethylene tubes sequentially every minute in the mixed return air duct and in nine rooms of the house including the attic. The GC–ECD was calibrated using an 18-point calibration system to measure  $\text{SF}_6$  concentrations between 30  $\mu\text{g}/\text{m}^3$  (5 ppb) and 900  $\mu\text{g}/\text{m}^3$  (150 ppb) with an accuracy of approximately  $\pm 2\%$ . Air change rates were calculated regressing the logarithm of the tracer gas concentration vs time. The fit normally achieved better than 98%  $R^2$  values, and the relative standard deviation (RSD) of the air change rates across the eight conditioned areas averaged less than 15%. With the central fan on, it takes about 30 min for all

rooms to achieve equilibrium tracer gas concentrations after an initial injection into the return duct. Therefore, the regression was carried out for 1 h, beginning 30 min after completion of the injection. The central fan was normally kept on at all times to allow the tracer gas in the duct to be distributed throughout the house. With the fan on, approximately 5 house volumes of air were forced through the ducts every hour, thus ensuring good mixing throughout the house. For the relatively few periods when the central fan was off, it was not possible to determine the air change rate using this method. The effect of the central fan on air change rates was tested and found to be nil. Since the ductwork was completely contained within the conditioned space (not entering the attic), there was no opportunity for leakage of air to the outdoors.

Two types of in-duct filters were tested during the year 2000 and were in operation during some of the 44 cooking episodes. One was an electrostatic precipitator (ESP), and the other was a fibrous mechanical filter (MECH). The ESP positively charges particles with ionizing wires at 6200 V. The charged particles are then removed by ground collector plates. The ESP required approximately monthly cleaning to maintain high removal efficiencies. The MECH has an extended surface area with a thickness of 0.13 m. The manufacturers' stated average arrestance was 93% per ASHRAE Standard 52.1 (19).

Each type of filter was installed at different times in the return duct. Probes were placed in the duct upstream and downstream from the filter. Two OPCs were attached to the probes to determine the efficiency of the filters for fine and coarse particles. (No measure of efficiency was attempted for ultrafine particles.) Since efficiencies approached 99% for the larger particle sizes, it is felt that filter leaks or bypass problems were minimal.

The main type of cooking studied here is frying. Ten cooking episodes involved frying flour tortillas in peanut oil at a depth of approximately 1 cm. The oil is allowed to get to the point of smoking, and the tortillas are placed in it for 5–10 s. This cooking procedure also usually involved heating the fried tortillas together with refried beans and Monterey jack cheese in the gas oven for approximately 4 min. Another type of cooking included here was stir-frying in a wok. For this type of cooking, a small amount of peanut oil was added to the wok, heated with garlic and ginger, and then brought to a high heat, and vegetables were added and stirred for approximately 5 min. A third type of cooking investigated was frying eggs in butter. About 15  $\text{cm}^3$  (1 Tbsp) of butter was melted in a frying pan, and 2–3 eggs were fried at medium heat for about 5 min. Three of the 24 episodes involved frying eggs. Other types of cooking included sautéing Swiss chard in a frying pan on a burner and grilling veggie burgers in a frying pan on a burner. Eight episodes involved more complex cooking processes including at least two different operations (e.g., frying on the stovetop burners plus some other operation such as boiling water or using the oven).

As has been previously noted (20–21), the gas flame itself produces ultrafine particles. We performed several tests with one, two, three, or four burners on at once but with no pot or pan or food being cooked. Large numbers of ultrafine particles were produced, with a peak near or below our smallest diameter of 9.8 nm. We noted also that the electric toaster oven could produce ultrafine particles peaking at about 30 nm when no bread was inserted. For the most part, these combustion activities without involving food produced few particles greater than 0.1  $\mu\text{m}$  in diameter. The addition of pans, food, and more complex cooking modes resulted in moving the peak to higher diameters, ranging up to 60 nm, and also in creating many particles in the accumulation mode (0.1–1  $\mu\text{m}$ ) and additional particles in the fine mode (1–2.5  $\mu\text{m}$ ).

**Source Strength Calculations.** To calculate source strengths, we employ the mass balance differential equation

$$dC_{in}/dt = PaC_{out} - (a + K)C_{in} + S/V \quad (1)$$

where  $C_{in}$  = indoor number or volume concentration ( $\text{cm}^{-3}$  or  $(\mu\text{m}/\text{cm})^3$ ),  $C_{out}$  = outdoor number or mass concentration,  $P$  = penetration coefficient across building envelope,  $a$  = air exchange rate ( $\text{h}^{-1}$ ),  $V$  = volume of building ( $400 \times 10^6 \text{ cm}^3$ ),  $S$  = source strength ( $\text{h}^{-1}$  or  $\mu\text{m h}^{-1}$ ), and  $K$  = total decay rate of particles ( $\text{h}^{-1}$ ). Here  $K = k + k_{HAC} + k_{filter}$ , where  $k$  is the natural decay rate of the particles when the central furnace fan is off,  $k_{HAC}$  is the additional decay rate when the fan is on (due to the fan forcing particles through the duct and HAC system as well as increasing the air turbulence in the rooms), and  $k_{filter}$  is the further decay due to the MECH or ESP (14, 15).

It is understood that the equation refers to a particular aerosol size, and that  $P$ ,  $K$ , and  $S$  may all be functions of particle size. This implies further that we are ignoring coagulation and condensation, processes that lead to changes in particle size. (Although coagulation may occur at the high concentrations encountered in the kitchen, by the time the aerosol mixture has reached the measuring instruments in rooms other than the kitchen, the concentration drops below that required for substantial coagulation.)

We make the additional assumptions of constant outdoor concentration over the course of the cooking episode and subsequent particle decay, as well as constant values for  $P$ ,  $a$ ,  $K$ , and  $S$  during the time of cooking. Furthermore, the house is considered to be a single well-mixed zone with instantaneous mixing. Finally, at the time of the beginning of the cooking, the conditions are considered to have held long enough before that to reach equilibrium. Under these conditions, the solution to the differential equation just before cooking begins ( $t = 0^-$ ,  $S = 0$ ) is simply

$$C_{in}(0^-) = PaC_{out}/(a + K) \quad (2)$$

After cooking begins, the general solution to the homogeneous form of eq 1 is

$$C_{in} = A \exp(-(a + K)t)$$

and a specific solution to the inhomogeneous form of eq 1 is

$$C_{in} = PaC_{out}/(a + K) + S/\{V(a + K)\}$$

We solve for the constant of integration  $A$  by requiring the solution just after cooking begins ( $t = 0^+$ ) to equal the solution just before cooking begins ( $t = 0^-$ ):

$$\begin{aligned} C_{in}(0^+) = \\ A + PaC_{out}/(a + K) + S/\{V(a + K)\} = PaC_{out}/(a + K) \\ A = -S/\{V(a + K)\} \end{aligned}$$

The general solution is then

$$\begin{aligned} C_{in}(t) = \\ PaC_{out}/(a + K) + (S/\{V(a + K)\})(1 - \exp(-(a + K)t)) \end{aligned} \quad (3)$$

The contribution of cooking at any time  $t$  to the indoor number or mass concentration is

$$\begin{aligned} \Delta C_{in}(t) = \\ C_{in}(t) - C_{in}(0) = (S/\{V(a + K)\})(1 - \exp(-(a + K)t)) \end{aligned}$$

Solving for  $S$

$$S = V(a + K)\Delta C_{in}/\{1 - \exp(-(a + K)t)\} \quad (4)$$

The criteria for selecting a cooking episode for study were (1) a sharp increase over background of at least a factor of 3 (the increase for specific particle sizes sometimes exceeded 2 orders of magnitude), (2) a return to baseline (indicating no change in outdoor concentrations), and (3) a smooth decay (indicating no other significant indoor sources active). An example of a particular cooking episode is supplied in Figure 1 to show the increase in concentration followed by a smooth decay.

These criteria resulted in the selection of 44 cooking episodes (24 for ultrafine and fine particles from 0.01 to 0.37  $\mu\text{m}$ , and 20 for the larger fine particles in the range of 0.5–2.5  $\mu\text{m}$ ), distributed over the three measurement methods as follows: DMA-CPC ( $N = 24$ ); APC ( $N = 9$ ); OPC ( $N = 11$ ).

In each case, the procedure for determining the source strength was as follows: (1) Determine the decay rate for the given particle size. This is done by determining the background concentration, subtracting the background from all of the elevated values following cooking, transforming to logarithms, and carrying out a regression analysis over time. Typically, decay curves lasted for 1–4 h, allowing at least 1 dozen to 4 dozen points on the curve to contribute to the regression. The negative slope of the regression is  $a + K$ . Regressions were required to achieve  $R^2$  values of 95% to be considered valid. (2) The peak concentration at each particle size was found, and the time to reach that peak from the most recent previous concentration less than half the peak size was determined. This time period, which corresponded to the greatest rate of increase in concentration, was typically 5–15 min. The maximum change in the basement concentration due to cooking ( $\Delta C$ ) was determined, and a mean source strength  $S$  (particles/h or particle volume/h) during this period was calculated from eq 4.

**DMA-CPC.** Twenty-four cooking episodes between July 2, 1999 and March 10, 2000 were selected, on the basis of the criteria above. The decay rates for each of the 102 particle sizes between 9.8 and 372 nm were determined.

**APC.** Nine cooking episodes between Oct 29, 1999 and June 30, 2000 were selected for analysis. The decay rates for each of the 22 particle sizes between 0.54 and 2.46  $\mu\text{m}$  were determined. Limited data were available for larger particle sizes, since the high gravitational settling rates of these larger particles remove them from the air before a well-mixed concentration is achieved.

**OPC.** The 11 separate cooking episodes included in our companion paper on deposition rates (14) were selected for analysis. In addition to the criteria above, criteria for selection included having at least two OPCs in different rooms with decay rates within 10% of each other. Since several OPCs were deployed in different rooms and floors of the home, a total of 19 determinations of the source strength were made from different OPCs used during the 11 cooking episodes. Only the OPCs located in rooms other than the kitchen were used in these calculations, since the peak values in the kitchen occurred before the particles were well mixed throughout the house. The decay rates and source strengths were determined for the three smallest particle size categories: 0.3–0.5, 0.5–1, and 1–2.5  $\mu\text{m}$ .

Because of the broadness of the OPC size categories, the selection of a "representative" particle diameter from which to calculate particle volumes can have a large effect on the calculated volume. However, in many of these cases, the collocated APC provided information on particle numbers at finer resolution, and an "equivalent" particle diameter could be chosen. If we assume that the number distribution as measured by the APC also applies to the concurrent and

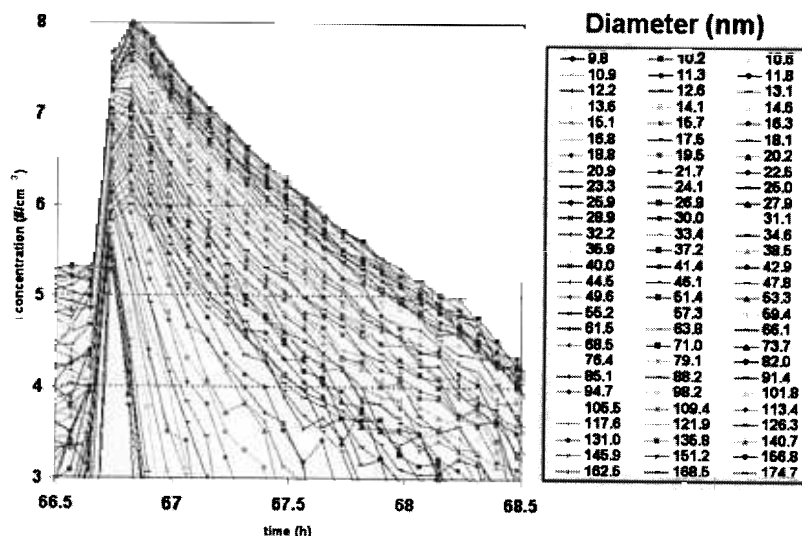


FIGURE 1. Example of a cooking episode as measured by the DMA-CPC for ultrafine particles. Points shown are at 5 min intervals.

colocated OPC measurements, then we can calculate an equivalent diameter for each OPC measurement to be used in calculating the total volume. The proper diameter to use is that equivalent diameter  $D_{eq}$  that provides the same volume (when multiplied by  $N$ ) as the integral or summation of the volumes of the particles within that size range:

$$ND_{eq}^3 = \sum N_i D_i^3 \quad (5)$$

where  $i$  indexes all of the smaller size subranges within the size range under consideration. Normally there is no way of knowing the values of  $N_i$ , but fortunately, in this case we have an APC with reasonably closely spaced subranges running concurrently with the OPC that was located in the basement. Therefore, for each of the measurements made by the APC, we calculated the  $D_{eq}$  corresponding to each of the OPC size bins (except for the 0.3–0.5  $\mu\text{m}$  bin) from eq 5. Then we used the calculated value of  $D_{eq}$  to obtain the equivalent volume. This concept of equivalent diameter is explained more fully in ref 16. For example, in the absence of any concurrent APC or other high-resolution size-specific data, a reasonable equivalent diameter for the 0.5–1  $\mu\text{m}$  size range might be the geometric mean (0.707  $\mu\text{m}$ ), but in fact the actual average equivalent diameter for the chosen cooking episodes was 0.545  $\mu\text{m}$ . Using the geometric mean would have led to a calculated volume more than twice the volume calculated using the equivalent diameter.

## Results

**Instrument Uncertainty.** Despite the manufacturers' calibrations of multiple OPC instruments at one time, side-by-side comparisons revealed biases between instruments ranging from 10% to 40% depending on the particle size channel being compared. These biases were minimized by selecting one instrument at random and correcting all other instruments to that reading. After the bias was removed in this way, residual differences between OPC instruments (precision) were lowest for the smallest size channel (0.3–0.5  $\mu\text{m}$ ) at about 2–3%, increasing to about 5% for the second largest channel (0.5–1  $\mu\text{m}$ ) and about 20% for the third largest (1–2.5  $\mu\text{m}$ ). For two OPC instruments in the basement, Spearman correlation coefficients were 0.94, 0.93, and 0.91 for the three size ranges 0.3–0.5, 0.5–1, and 1–2.5  $\mu\text{m}$  ( $N = 7476$ ).

The APC and OPC were compared to each other for all times during which they were colocated in the January to

May 2000 period. The mean fine particle ( $\text{PM}_{2.5}$ ) volumes measured by the OPC and APC when an indoor source was operating were 2.70 and 2.83 ( $\mu\text{m}/\text{cm}^3$ ) ( $N = 5023$  5 min average values). Corresponding volumes with no indoor source were 0.77 and 0.71 ( $\mu\text{m}/\text{cm}^3$ ) ( $N = 9777$ ). Although this is good agreement overall, agreement was worse for the individual size categories, suggesting that the category cutpoints differed between the two instruments.

Spearman correlations were calculated between the three OPC size ranges below 2.5  $\mu\text{m}$  and the corresponding size ranges of the APC for the five months that both were operating in the basement. When no indoor source was operating, the correlation coefficients for the 0.3–0.5, 0.5–1, and 1–2.5  $\mu\text{m}$  categories were 0.90, 0.82, and 0.76, respectively ( $N = 11\,880$ ). When an indoor source was operating, the respective coefficients were 0.90, 0.75, and 0.69 ( $N = 6880$ ).

Since only one DMA-CPC was available, it was not possible to determine precision, nor, since no other instrument was measuring ultrafine particles, was it possible to determine agreement with other instruments. The DMA is considered as a reference instrument for determining particle sizes by the National Institute for Standards and Materials; thus, we can be confident that the size categories are correct. However, the concentration estimates within those categories could not be verified within this study. Errors could occur in the internal voltage settings determining the split air flows and the total air flow. The internal voltage settings were adjusted before each monitoring episode to within 0.1% of the recommended values, and the total air flow was measured by a flow meter to within 0.3% of the recommended value. Air flow rates at the end of the monitoring periods showed minimal drift, on the order of 1%. If the particles were not fully charged by the radioactive device, errors could result from not achieving Boltzmann equilibrium; these errors depend on the aerosol distribution but could result in overall errors of about 5%.

**Deposition Rates.** The mean values of  $a + K$  for the 24 cooking events measured by the DMA-CPC and the 9 cooking events measured by the APC are shown in Figure 2 as a function of particle diameter. The general "U" shape of the curve is in agreement with theoretical expectations (22) and experimental findings (14, 15). The smallest particles deposit more rapidly due to Brownian motion, and the largest particles deposit more rapidly due to gravitation. The minimum depends partly on indoor air velocity but is expected to occur near 0.1  $\mu\text{m}$ . Note that these values include

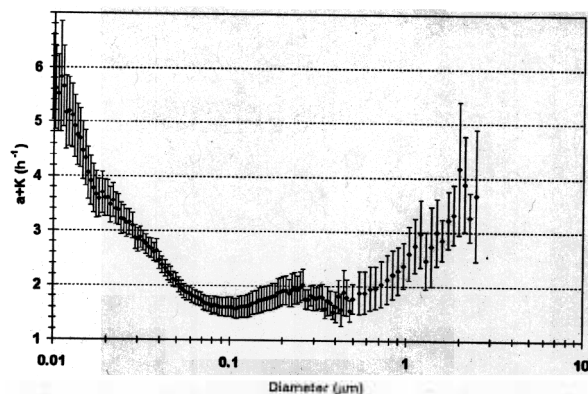


FIGURE 2. Mean values of  $a + K$  as a function of particle diameter for the 24 cooking events measured by the DMA-CPC and the 9 events measured by the APC. Error bars are  $\pm 1$  standard error.

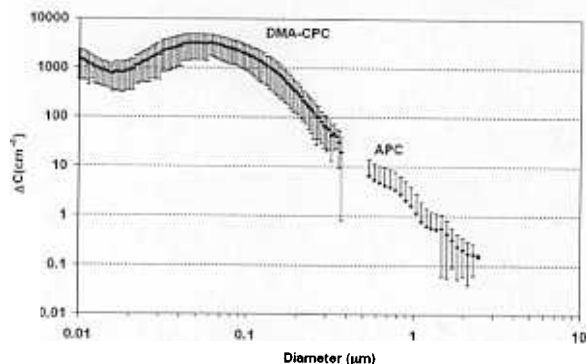


FIGURE 3. Observed arithmetic mean number concentration of particles between 10 nm and 2.46  $\mu\text{m}$  due to cooking on a gas stove (measurements in the basement, cooking in the kitchen). Error bars are standard deviations. (Missing lower error bars correspond to standard deviations that are larger than the mean and thus cannot be plotted on a logarithmic scale.) Twenty-four cooking episodes are included for the DMA-CPC (particle diameters between 0.01 and 0.33  $\mu\text{m}$ ); nine episodes are included for the APC (particle diameters between 0.54 and 2.46  $\mu\text{m}$ ).

some periods with air filters working and some without, leading to considerable variation in the values of  $K$ . Air change rates ranged between 0.09 and 1.25  $\text{h}^{-1}$ , with a mean (SD) of 0.39 (0.26)  $\text{h}^{-1}$ .

**Distributions of Number Concentrations, Source Strengths, and Volume Concentrations.** The number concentration distribution as a function of particle size has a clear bimodal distribution with a peak (1500 particles/ $\text{cm}^3$ ) at or below 0.01  $\mu\text{m}$  and a second peak (3300 particles/ $\text{cm}^3$ ) at about 0.06  $\mu\text{m}$  (Figure 3). The intervening minimum (of about 750 particles/ $\text{cm}^3$ ) occurs at about 0.016  $\mu\text{m}$ . The concentration declines steadily, falling below 1 particle/ $\text{cm}^3$  at diameters  $> 1 \mu\text{m}$ .

The source strength calculated from these observed number concentrations has a nearly identical bimodal distribution, with a peak of  $5 \times 10^{12}$  particles/h at 0.01  $\mu\text{m}$ , a local minimum of  $2.5 \times 10^{12}$  particles/h at 0.016  $\mu\text{m}$ , and a second peak of almost  $10^{13}$  particles/h at a particle diameter of 0.06  $\mu\text{m}$ . The source strength exceeds  $10^{12}$  particles/h up to about 0.2  $\mu\text{m}$ , declines to  $10^{11}$  particles/h at the extreme of the DMA-CPC range (0.37  $\mu\text{m}$  in this study), and ranges downward from  $2.5 \times 10^{10}$  particles/h at 0.5  $\mu\text{m}$  to less than  $10^9$  particles/h at 2.46  $\mu\text{m}$  (Figure 4).

The volume distribution ranges over 3 orders of magnitude, beginning at  $< 0.001 (\mu\text{m}/\text{cm})^3$  for the smallest ultrafine particles, reaching a local maximum of about  $1.5 (\mu\text{m}/\text{cm})^3$

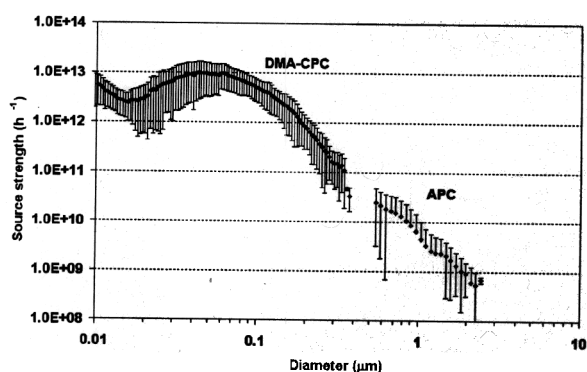


FIGURE 4. Mean source strength (particles/h) and associated standard deviations for the 33 cooking episodes employing the DMA-CPC and the APC.

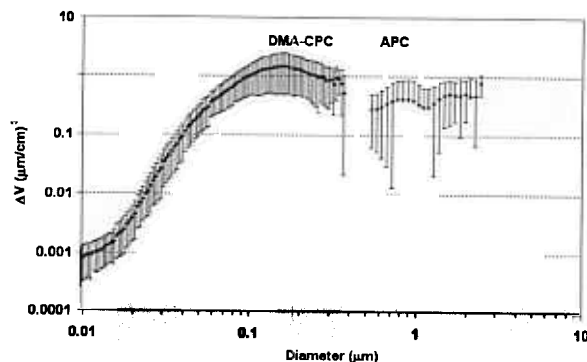


FIGURE 5. Mean volume distribution and associated standard deviations of ultrafine and fine particles due to cooking on a gas stove.

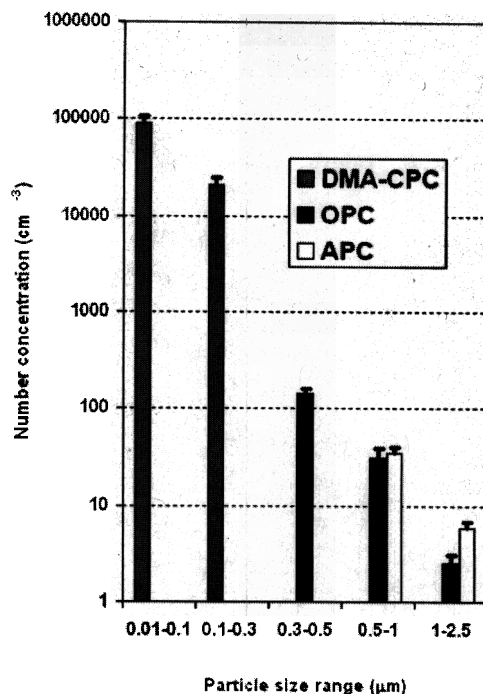


FIGURE 6. Mean numbers of particles produced by 44 cooking episodes on a gas stove. Error bars are standard errors.

at about 0.16  $\mu\text{m}$ , and falling below 1  $(\mu\text{m}/\text{cm})^3$  at about 0.28  $\mu\text{m}$  (Figure 5). The volumes recorded by the APC ranged between 0.2 and 0.8  $(\mu\text{m}/\text{cm})^3$  for all particle sizes.



TABLE 1. Number and Volume Concentrations of All Cooking Episodes during the Year 2000 Compared to Concentrations at the Same Times without Cooking

size (μm)	dinner			no cooking 6–10 p.m.			breakfast			no cooking 6–10 a.m.			dinner ratio <sup>c</sup>	breakfast ratio <sup>d</sup>
	N <sup>a</sup>	mean	SE	N <sup>b</sup>	mean	SE	N	mean	SE	N	mean	SE		
Number (cm <sup>-3</sup> )														
0.010–0.018	3714	6472	165	4623	465	10	2415	4558	141	6148	352	7	13.9	12.9
0.018–0.05	3714	13363	342	4623	1507	22	2415	5795	158	6148	662	10	8.9	8.8
0.05–0.1	3714	7085	221	4623	1701	29	2415	1547	61	6148	626	7	4.2	2.5
0.1–0.2	3714	2226	77	4623	807	11	2415	572	11	6148	437	5	2.8	1.3
0.2–0.3	3714	277	10	4623	128	1.4	2415	107	6	6148	86	1.1	2.2	1.2
0.3–0.5	4587	76	3	10679	16	0.15	2670	77	3	12856	13	0.15	4.8	5.7
0.5–1	4588	5	0.086	10679	1.3	0.015	2670	4.3	0.09	12856	1	0.011	3.8	3.7
1–2.5	4588	1	0.016	10679	0.15	0.0016	2670	0.8	0.04	12856	0.11	0.001	4.5	7.5
Volume (μm/cm) <sup>3</sup>														
0.010–0.018	3714	0.0085	0.0002	4623	0.0006	0.00001	2415	0.0059	0.0002	6148	0.0005	0.00001	14.0	12.8
0.018–0.05	3714	0.3	0.01	4623	0.039	0.0006	2415	0.1	0.003	6148	0.015	0.0002	7.4	6.8
0.05–0.1	3714	1.4	0.04	4623	0.4	0.006	2415	0.3	0.01	6148	0.14	0.001	3.8	2.1
0.1–0.2	3714	2.9	0.10	4623	1.1	0.014	2415	0.8	0.02	6148	0.64	0.007	2.6	1.3
0.2–0.3	3714	2.6	0.12	4623	1.2	0.013	2415	1.1	0.09	6148	0.79	0.010	2.3	1.4
0.3–0.5	4587	2.4	0.05	10679	0.5	0.005	2670	2.6	0.10	12856	0.45	0.005	4.6	5.8
0.5–1	4588	0.8	0.01	10679	0.2	0.003	2670	0.7	0.02	12856	0.18	0.002	3.8	3.8
1–2.5	4588	1.4	0.04	10679	0.3	0.003	2670	1.8	0.12	12856	0.20	0.002	4.9	9.4
sum (PM <sub>2.5</sub> )		11.8			3.7			7.4			2.4		3.2	3.1

<sup>a</sup> Number of 5 min periods between 6 and 10 p.m. associated with elevated concentrations due to cooking. <sup>b</sup> Number of 5 min periods between 6 and 10 p.m. without elevated concentrations due to cooking. <sup>c</sup> Ratio of mean concentration while cooking dinner to mean concentration when no cooking occurs during the 6–10 p.m. time period. <sup>d</sup> Ratio of mean concentration while cooking breakfast to mean concentration when no cooking occurs during the 6–10 a.m. time period.

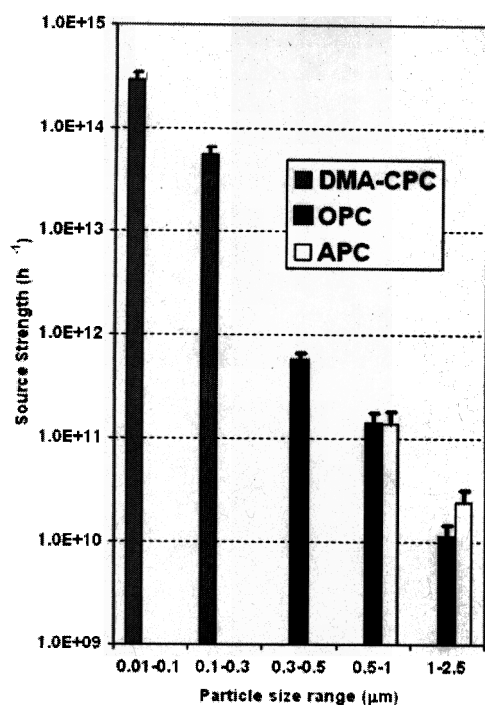


FIGURE 7. Mean source strengths of particles from 44 cooking episodes on a gas stove.

**Summed Distributions by Particle Class.** These observed distributions were summed into five categories: ultrafine particles ( $<0.1 \mu\text{m}$ ), accumulation mode particles measured by the DMA-CPC ( $0.1-0.3 \mu\text{m}$ ), accumulation mode particles measured by the OPC ( $0.3-0.5 \mu\text{m}$ ) and by the OPC and APC ( $0.5-1 \mu\text{m}$ ), and fine particles ( $1-2.5 \mu\text{m}$ ) measured by the OPC and APC. The concentrations in each category show a monotonic decline with increasing particle diameter, from 100 000 ultrafine particles/ $\text{cm}^3$  to less than 10 fine particles/ $\text{cm}^3$  (Figure 6).

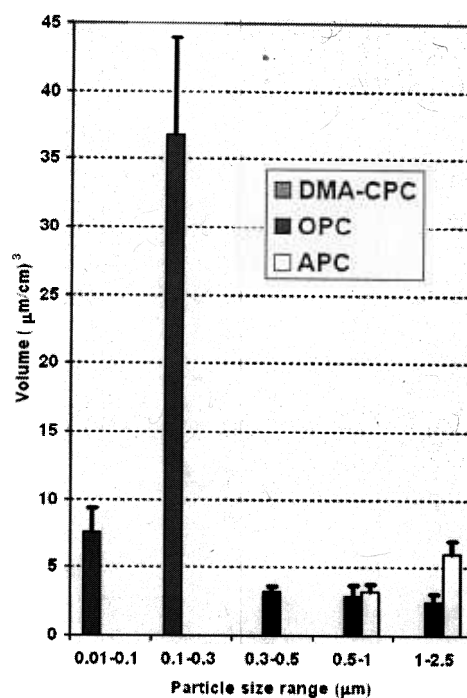


FIGURE 8. Mean volumes of particles produced by 44 cooking episodes on a gas stove.

The associated source strengths (Figure 7) range from  $2 \times 10^{14} \text{ h}^{-1}$  for the ultrafine particles to about  $10^{10} \text{ h}^{-1}$  for the fine particles ( $1-2.5 \mu\text{m}$ ). (Although individual particle sizes had a maximum source strength of only  $10^{13} \text{ h}^{-1}$  (Figure 4), recall that we are summing across more than 20 such size categories to produce the first bar in Figure 7.)

The particle volumes produced by the 44 cooking episodes show a strong peak in the  $0.1-0.3 \mu\text{m}$  category, with over half the total volume of  $50 \mu\text{m}/\text{cm}^3$  occurring in that category (Figure 8).

**Comparison of High-Production Cooking Episodes with All Types of Cooking.** The cooking episodes studied were selected because they produced sufficient particles to obtain a reasonable estimate of the decay rate, which in turn allows calculation of the source strength; therefore, they are not representative of all cooking types. Even considering only frying and sautéing, these events are probably above average in the amount of particles produced. Therefore, the absolute numbers reported here may be overestimates of average cooking source strengths.

We can arrive at an estimate of the number concentrations and particle volumes due to all types of cooking by a more general procedure. We consider the measurements made over the entire year 2000. All times of increased particle concentrations due to cooking were identified, adding up to about 300–400 h at dinnertime and 200 h at breakfast time. By taking the breakfast period between 6 a.m. and 10 a.m., and the dinner period between 6 p.m. and 10 p.m., and calculating the increase over the noncooking background of the particle numbers during those periods, we can arrive at an estimate of the average increase due to cooking of all types. The total particle number and volume concentrations during cooking were about 3 times the levels when no cooking occurred (Table 1).

## Discussion

We find that 44 high-particle-production cooking episodes on a gas stove created particles at the rate of about  $10^{14}$  particles/h over a typical cooking time of about 5–15 min. Most of the particles are in the ultrafine range, but the largest volume is contributed by particles between 0.1 and  $0.3\ \mu\text{m}$  in diameter (Figure 8). The total particle volumes created by the 44 cooking events averaged a little more than  $50\ (\mu\text{m}/\text{cm})^3$ . We can translate these volumes to estimated mass concentrations by assuming a specific gravity of 1.0 for combustion particles (23). A volume of  $1\ (\mu\text{m}/\text{cm})^3$  would have a mass of  $1\ \mu\text{g}/\text{m}^3$ ; thus, the volume numbers can be directly viewed as rough estimates of mass. Therefore, the 44 selected cooking episodes produced an average concentration throughout the house of about  $50\ \mu\text{g}/\text{m}^3$ .

These concentrations, associated mostly with frying, are likely to be near the upper limit of most cooking modes. An estimate of average concentrations due to all modes of cooking is provided in Table 1, where we find that all types of dinnertime cooking throughout the year produced increases of about  $8\ \mu\text{g}/\text{m}^3$  and breakfast cooking produced smaller increases of about  $5\ \mu\text{g}/\text{m}^3$ , compared to background levels during the same time periods. This range of 5– $8\ \mu\text{g}/\text{m}^3$  is consistent with the average increase of  $6\ \mu\text{g}/\text{m}^3$  attributed to cooking in 178 homes in Riverside, CA (5).

Comparing to the  $50\ \mu\text{g}/\text{m}^3$  of the selected cooking (mostly frying) episodes, we see that frying is capable of increasing the total particle production due to cooking by factors of 6–10. Although it is not possible to calculate source strengths for the hundreds of cooking episodes over the year due to inability to measure the deposition rates, if we assume a similar range of deposition rates, it would be reasonable to estimate that source strengths for these more representative cooking modes would be 6–10 times lower than the source strengths associated with frying.

Particle production during cooking is heavily weighted toward the ultrafine particles. The smallest ultrafines (10–18 nm) were elevated by factors of 13–14 over background, and the next smallest category (18–50 nm) by factors of 7–9, whether number or mass concentrations are the metric (Table 1). Cooking-related concentrations of the remaining submicrometer particle size categories were increased by factors ranging from 1.2 to 5.8.

Number and volume concentrations during the breakfast period were generally less than those during dinnertime.

Although part of this increase may have been due to the increased time of cooking, we also noted a shift toward larger sizes for the more complex dinnertime cooking. More than 80% of the particles were  $<0.05\ \mu\text{m}$  during the breakfast cooking compared to about 70% of the dinnertime particles.

Two previous studies (20, 21) provided useful data on ultrafine particle number concentrations during cooking. Both studies showed that the gas burner alone or an electric stovetop heating element alone could produce copious numbers of ultrafine particles even in the absence of pots, water, or food being cooked. Both studies noted that the particle production during these noncooking events was limited largely to ultrafine particles, with few particles being created  $>0.1\ \mu\text{m}$  in diameter. Both studies also provided useful data on number and volume concentrations associated with different types of cooking, but neither study made the measurements of particle deposition rates required to estimate source strengths.

Two more complete investigations of particle number and volume concentrations due to cooking are available as reports but have not been published in peer-reviewed journals (24, 25). One of these (24) employed an OPC with 16 size bins from 0.09 to  $3.0\ \mu\text{m}$  in diameter. Since the lowest size cutoff in that study excluded the ultrafine particles with the largest number concentrations, the findings regarding number of particles are not directly comparable. However, most of the fine particles produced by cooking were less than  $0.5\ \mu\text{m}$ , in agreement with our findings.

A study sponsored by the California Air Resources Board (25) employed an electrical mobility particle monitor with 12 size bins from 0.03 to  $10\ \mu\text{m}$  in diameter. Although this monitor extends further into the ultrafine range than the OPC used in ref 24, it still fails to sample the sizes (0.01– $0.03\ \mu\text{m}$ ) making the highest contribution to the total number of particles, and thus, the findings regarding number of particles are again not directly comparable to our findings. The investigators also collected particles on filters using a low-flow  $\text{PM}_{2.5}$  monitor. One of these experiments included frying tortillas in oil on a gas stove and is thus comparable to some of our own experiments. Mean gravimetric concentrations in the bedroom of the uninhabited house used for these experiments reached  $77\ \mu\text{g}/\text{m}^3$ , compared to our estimated mean peak concentration in the basement of about  $50\ \mu\text{g}/\text{m}^3$ . The cooking time was longer and the house was smaller in the CARB study, both of which would lead to higher concentrations. In that study, the investigators calculated an energy use of 5000 kJ (4700 Btu) for the tortilla cooking experiment and a corresponding  $\text{PM}_{2.5}$  source strength of  $38\ \mu\text{g}/\text{kJ}$  ( $40\ \mu\text{g}/\text{Btu}$ ). For our tortilla experiments, the energy use was about 2100 kJ (2000 Btu) (one burner on for about 10 min and the oven on for about 4 min), leading to a source strength of about  $10\ \mu\text{g}/\text{kJ}$  ( $10\ \mu\text{g}/\text{Btu}$ ).

These calculations of source strengths per time of cooking or per energy used have quite wide uncertainties, due to different methods of cooking, different temperatures of the cooking oil, etc. Indoor air quality models employing the source strengths estimated here or in other studies will need to take into account this extreme variability. However, because the source strength estimates are independent of variables such as house volume, air change rates, and deposition velocities, they are more suitable for modeling purposes than the number or volume concentrations.

Since most particles were  $<0.1\ \mu\text{m}$  and most of the volume (mass) was contained in particles of  $<0.3\ \mu\text{m}$ , only air filters capable of removing such small particles would be effective in reducing particle number concentrations due to cooking. Our work with two types of in-duct air filters, a mechanical filter and an electrostatic precipitator, suggested that only the ESP was capable of removing particles smaller than  $1\ \mu\text{m}$  (14, 15). It could achieve efficiencies of 90% for particles

between 0.3 and 1  $\mu\text{m}$ , but needed consistent cleaning at monthly intervals to retain such high efficiency. Other types of mechanical filters (not tested in this study) may also be capable of effectively removing small particles.

### Acknowledgments

We acknowledge the contributions of Stuart Dols and Steven Nabinger of the National Institute of Standards and Technology in constructing, calibrating, and repairing the equipment. This study was partially funded by an EPA internal grant to the corresponding author. It was also supported by the National Institute of Standards and Technology. The paper has been reviewed by both agencies and cleared for publication. Certain commercial equipment, instruments, or materials are identified in this paper to specify the experimental procedure adequately. Such identification is not intended to imply recommendation or endorsement by the National Institute of Standards and Technology, nor is it intended to imply that the materials or equipment identified are necessarily the best available for the purpose.

### Literature Cited

- (1) National Academy of Sciences. *Research Priorities for Airborne Particulate Matter III. Early Research Progress*; National Academy Press: Washington DC, 2001.
- (2) Oberdorster, G.; Gelein, R. M.; Ferin, J.; Weiss, B. Association of particulate air pollution and acute mortality: involvement of ultrafine particles? *Inhalation Toxicol.* **1995**, *7*, 111–124.
- (3) Goldstein, B. D.; et al. The relationship between respiratory illness in primary school children and the use of gas for cooking: II. Factors affecting nitrogen dioxide levels in the home. *Int. J. Epidemiol.* **1979**, *8*, 339–345.
- (4) Seaton, A.; Dennekamp, M. Hypothesis: Ill health associated with low concentrations of nitrogen dioxide—an effect of ultrafine particles? *Thorax* **2003**, *58*, 1012–1015.
- (5) Özkaynak, H.; Xue, J.; Spengler, J. D.; Wallace, L. A.; Pellizzari, E. D.; Jenkins, P. Personal exposure to airborne particles and metals: results from the Particle TEAM Study in Riverside, CA. *J. Exposure Anal. Environ. Epidemiol.* **1996**, *6*, 57–78.
- (6) Özkaynak, H.; Xue, J.; Weker, R.; Butler, D.; Koutrakis, P.; Spengler, J. *The Particle TEAM (PTEAM) Study: Analysis of the Data. Volume 3*; EPA/600/R-95/098; U.S. Environmental Protection Agency: Research Triangle Park, NC, 1996.
- (7) Wallace, L. A. Indoor particles: A review. *J. Air Waste Manage. Assoc.* **1996**, *46*, 98–126.
- (8) Wallace, L. A.; Mitchell, H.; O'Connor, G. T.; Liu, L.-J. S.; Neas, L.; Lippmann, M.; Kattan, M.; Koenig, J.; Stout, J. W.; Vaughn, B. J.; Wallace, D.; Walter, M.; Adams, K. Particle concentrations in inner-city homes of children with asthma: the effect of smoking, cooking, and outdoor pollution. *Environ. Health Perspect.* **2003**, *111*, 1265–1272.
- (9) Abt, E.; Suh, H. H.; Catalano, P.; Koutrakis, P. 2000. Relative contribution of outdoor and indoor particle sources to indoor concentrations. *Environ. Sci. Technol.* **2000**, *34*, 3579–3587.
- (10) Long, C. M.; Suh, H. H.; Catalano, P.; Koutrakis, P. Using time- and size-resolved particulate data to quantify indoor penetration and deposition behavior. *Environ. Sci. Technol.* **2001**, *35*, 2089–2099.
- (11) Vette, A. F.; Rea, A. W.; Lawless, P. A.; Rodes, C. E.; Evans, G.; Highsmith, V. R.; Sheldon, L. Characterization of indoor-outdoor aerosol concentration relationships during the Fresno PM exposure studies. *Aerosol Sci. Technol.* **2001**, *34*, 118–126.
- (12) Howard-Reed, C. H.; Wallace, L. A.; Ott, W. R. The effect of opening windows on air change rates in two homes. *J. Air Waste Manage. Assoc.* **2002**, *52*, 147–159.
- (13) Wallace, L. A.; Emmerich, S. J.; Howard-Reed, C. Continuous measurements of air change rates in an occupied house for 1 year: The effect of temperature, wind, fans, and windows. *J. Exposure Anal. Environ. Epidemiol.* **2002**, *12*, 296–306.
- (14) Howard-Reed, C.; Wallace, L.; Emmerich, S. J. Effect of ventilation systems and air filters on decay rates of particles produced by indoor sources in an occupied townhouse. *Atmos. Environ.* **2003**, *37* (38), 5295–5306.
- (15) Wallace, L. A.; Emmerich, S. J.; Howard-Reed, C. Effect of central fans and in-duct filters on deposition rates of ultrafine and fine particles in an occupied townhouse. *Atmos. Environ.* **2004**, *38* (4), 405–413.
- (16) Wallace, L. A.; Howard-Reed, C. Continuous measurements of air change rates in an occupied house for 1 year: The effect of temperature, wind, fans, and windows. *J. Air Waste Manage. Assoc.* **2002**, *52*, 828–844.
- (17) Armendariz, A.; Leith, D. Concentration measurement and counting efficiency for the aerodynamic particle sizer 3320. *J. Aerosol Sci.* **2000**, *33*, 133–148.
- (18) ASTM. *Standard test method for determining air change in a single zone by means of a tracer gas dilution. E741-00*; American Society for Testing and Materials: West Conshohocken, PA, 2001.
- (19) ASHRAE. *Gravimetric and dust spot procedures for testing air cleaning devices used in general ventilation for removing particulate matter*; Standard 52.1; American Society of Heating, Refrigerating, and Air-Conditioning Engineers, Inc., 1992.
- (20) Dennekamp, M.; Howarth, S.; Dick, C. A.; Cherrie, J. H. W.; Donaldson, K.; Seaton, A. Ultrafine particles and nitrogen oxides generated by gas and electric cooking. *Occup. Environ. Med.* **2001**, *58*, 511–516.
- (21) Wallace, L. A. Real-time monitoring of particles, PAH, and CO in an occupied townhouse. *Appl. Occup. Environ. Hyg.* **2000**, *15*, 1–9.
- (22) Lai, A. C. K.; Nazaroff, W. W. Modeling indoor particle deposition from turbulent flow onto smooth surfaces. *J. Aerosol Sci.* **2000**, *31*, 463–476.
- (23) Sioutas, C.; Kim, S.; Chang, M. C.; Terrell, L. L.; Gong, H. Field evaluation of a modified DataRAM MIE scattering monitor for real-time PM<sub>2.5</sub> mass concentration measurements. *Atmos. Environ.* **2000**, *34*, 4829–4838.
- (24) Kelly, T. *Measurement of particulate and vapor emissions from cooking activities: final report (June 1998 – June 2001)*; Contract No. 5083; Gas Research Institute: Des Plaines, IL, 2001.
- (25) Fortmann, R.; Karlier, P.; Clayton, R. *Indoor air quality: residential cooking exposures. Final report*; California Air Resources Board Contract No. 97-330; Air Resources Board: Sacramento, CA, 2002.

Received for review September 15, 2003. Revised manuscript received January 21, 2004. Accepted January 27, 2004.

ES0306260